Eur Radiol (2018) 28:1054–1065
DOI 10.1007/s00330-017-5000-z

COMPUTED TOMOGRAPHY

Assessment of CT dose to the fetus and pregnant female patient using patient-specific computational models

Tianwu Xie[1] · **Pierre-Alexandre Poletti**[1] · **Alexandra Platon**[1] · **Christoph D. Becker**[1] · **Habib Zaidi**[1,2,3,4,5]

Received: 17 May 2017 / Revised: 4 July 2017 / Accepted: 21 July 2017 / Published online: 8 September 2017

Abstract

Purpose This work provides detailed estimates of the foetal dose from diagnostic CT imaging of pregnant patients to enable the assessment of the diagnostic benefits considering the associated radiation risks.

Materials and methods To produce realistic biological and physical representations of pregnant patients and the embedded foetus, we developed a methodology for construction of patient-specific voxel-based computational phantoms based on existing standardised hybrid computational pregnant female phantoms. We estimated the maternal absorbed dose and foetal organ dose for 30 pregnant patients referred to the emergency unit of Geneva University Hospital for abdominal CT scans.

Results The effective dose to the mother varied from 1.1 mSv to 2.0 mSv with an average of 1.6 mSv, while commercial dose-tracking software reported an average effective dose of 1.9 mSv (range 1.7–2.3 mSv). The foetal dose normalised to $CTDI_{vol}$ varies between 0.85 and 1.63 with an average of 1.17.

Conclusion The methodology for construction of personalised computational models can be exploited to estimate the patient-specific radiation dose from CT imaging procedures. Likewise, the dosimetric data can be used for assessment of the radiation risks to pregnant patients and the foetus from various CT scanning protocols, thus guiding the decision-making process.

Key points

- *In CT examinations, the absorbed dose is non-uniformly distributed within foetal organs.*
- *This work reports, for the first time, estimates of foetal organ-level dose.*
- *The foetal brain and skeleton doses present significant correlation with gestational age.*
- *The conceptus dose normalised to $CTDI_{vol}$ varies between 0.85 and 1.63.*
- *The developed methodology is adequate for patient-specific CT radiation dosimetry.*

Keywords CT · Radiation dosimetry · Foetal dose · Pregnant female models · Monte Carlo simulation

Electronic supplementary material The online version of this article (doi:10.1007/s00330-017-5000-z) contains supplementary material, which is available to authorized users.

✉ Habib Zaidi
habib.zaidi@hcuge.ch

[1] Department of Medical Imaging and Information Sciences, Geneva University Hospital, Geneva, Switzerland

[2] Geneva Neuroscience Center, Geneva University, Geneva, Switzerland

[3] Department of Nuclear Medicine and Molecular Imaging, University of Groningen, University Medical Center Groningen, Groningen, The Netherlands

[4] Department of Nuclear Medicine, University of Southern Denmark, DK-500 Odense, Denmark

[5] Division of Nuclear Medicine and Molecular Imaging, Geneva University Hospital, CH-1211 Geneva, Switzerland

Introduction

Pregnant females represent a critical subpopulation for which absorbed doses from radiological imaging procedures must be evaluated to make critical decisions regarding the outcome of the developing foetus. Over the period 1997–2006, the number of CT examinations performed on pregnant patients in the USA has increased by over 400% [1]. A similar trend is also observed in molecular and hybrid imaging technologies [2, 3]. This increase has led to increasing health concerns regarding the radiation risks

to the foetus. Obviously, the best way to care about radiation protection of patients is to avoid radiation as much as possible. Alternative non-ionising imaging modalities, such as ultrasound (US) and magnetic resonance imaging (MRI), have to be considered first to diagnose the cause of symptoms. At foetal doses greater than 100 mGy, the potential hazard effects of radiation on the foetus include possible spontaneous abortion, intrauterine growth limitation, average intelligence quotient (IQ) loss, mental retardation, possible organ malformation and small head size [4]. Stochastic effects, such as cancer and organ-specific disease, might also occur at foetal doses below 50 mGy [5–7]. The foetal nervous system exhibits a longer period of sensitivity to ionising radiation than other foetal tissues and is also known to be affected by radiation exposure above 5 mGy [8]. The increased absolute incidence for childhood cancer is 0.017% per mGy [9], while the excess relative risk for leukaemia and brain tumours are 0.036 (95% confidence interval (CI) 0.005–0.120) and 0.023 per mGy (95% CI 0.0098–0.0494), respectively [10].

Accurate estimation of foetal absorbed dose and associated risk factors from CT examinations is highly desired owing to the high radiosensitivity of developing foetal organs. However, this constitutes an enormous challenge since direct measurements of energy deposition in the foetal body cannot be performed in human beings because of ethical and radiation protection issues, and alternative approaches using anthropomorphic phantoms can be used as a substitute [1]. Different approaches have been followed to estimate the foetal dose, including Monte Carlo simulations using computational anthropomorphic models [11–21] and measurements using physical phantoms with embedded dosimeters [22–26]. However, these approaches inherently bear a number of limitations, such as the difficulty of constructing patient-specific computational models and the difficulty of matching anthropomorphic physical phantoms to the size and location of the foetus within the maternal body [27]. Therefore, the assumptions inherent to the measurement and simulation setup might cause significant overestimation or underestimation of the foetal absorbed dose. While Monte Carlo calculations are considered as reference (gold standard) for dose estimation in diagnostic imaging [28], implementation of a framework for patient-specific estimation of foetal dose from CT examinations of pregnant patients in clinical setting is highly desired.

In this work, we propose a methodology for the construction of patient-specific computational models based on image segmentation and registration methods and previously developed standardised hybrid computational phantoms of pregnant female series [29]. The geometry of the Discovery CT 750 HD CT scanner (GE Healthcare, Waukesha, WI) was designed and integrated within the N-Particle eXtended (MCNPX) Monte Carlo code. The patient-specific maternal and foetal absorbed radiation doses were calculated and compared with the results provided by the Radimetrics™ (Bayer Healthcare) commercial dose-tracking software [30]. The correlation between patient anatomy, gestational age conceptus position and foetal organ-level dose from CT scans was investigated.

Materials and methods

Pregnant patient CT examinations

The institutional ethics committee approved this retrospective study. Written informed consent was waived. CT images of 30 pregnant patients referred to the emergency unit of Geneva University Hospital (HUG) for abdominal and pelvic CT imaging were included in the study protocol. US was systematically performed upon admission of every pregnant patient with acute abdominal pain. Further examination (MRI or CT) was obtained when US was either inconclusive or negative with a high clinical suspicion. Low-dose CT was performed when MRI was not immediately available. The studies were acquired on the GE 750HD CT scanner (120 kVp, slice thickness from 0.625 to 3 mm, pitch of 1.375, table speed of 55 mm/rot and 31.5 mAs tube current without current modulation corresponding to 22.9 effective mAs, i.e. mAs/pitch). Tube current modulation was not applied in this retrospective study approved by the ethics committee until the end of the initial study. All pregnant patients receiving low-dose CT scans (same tube current and $CTDI_{vol}$ of 1.8 mGy) between March 2011 and September 2015 were included. The 30 pregnant patients (age range: 19–45 years) had gestational ages ranging between 8 weeks and 35 weeks, with an average gestational age of 19 weeks. A representative CT slice of a pregnant patient is shown in Fig. 1a. The body contour, skeleton and lungs were automatically segmented using thresholding, whereas the uterus was manually identified (Fig. 1b). Thirty voxelised regional models corresponding to the axial scanned length of pregnant patients were created from the segmented CT image data of the maternal body, including skeleton, lung and uterus. The craniocaudal length of voxelised regional models of patients depends on the scanned length of CT image data and ranges at least from the lower thorax to the pubic symphysis of the patient's anatomy. The maternal perimeter and conceptus depth were measured automatically from the constructed regional voxel model for each patient using an in-house C++ code as shown in Fig. 1b. The maternal perimeter was determined by the maximum outer perimeter of the patient on the image containing the uterus while the conceptus depth was measured as the average distance from the skin to the closest surface of the uterus because it is difficult to segment the foetal body on low-dose CT images. These two measurements were used to estimate the size of the maternal body

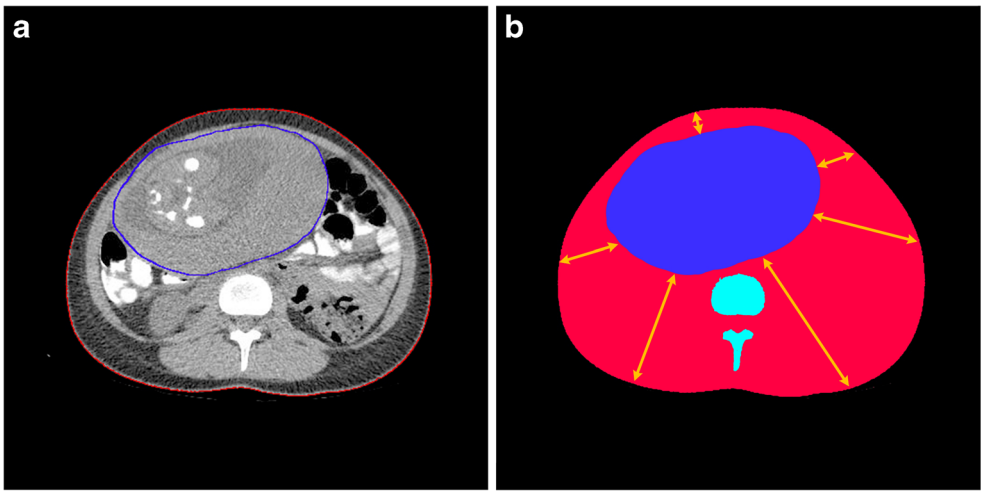

Fig. 1 (**a**) CT image with external body contour (red line) around the perimeter of a pregnant patient, the uterus (blue line) with a 29-week-old foetus. (**b**) Segmented CT image with external body contour, skeleton and uterus. The assessment of conceptus depth (averaged distance from skin to uterus [double arrow]) is also shown

and the location of the foetus within the mother's abdomen, respectively.

Patient-specific computational models

A series of ICRP-based standardised computational phantoms of pregnant females at the 8th, 10th, 15th, 20th, 25th, 30th, 35th and 38th weeks of gestations developed previously [29] were used as anchor models for the construction of patient-specific models. The corresponding anchor model of the closest gestational age was registered to the constructed voxelised regional patient-specific model using automatic affine registration to produce new personalised pregnant phantoms with well-defined anatomical structures, matching patient images obtained from CT examinations. The resulting models after registration are referred to as 'patient-specific computational models' below. Image registration was performed using the Insight Toolkit (ITK) [31]. Figure 2 shows two representative examples of the patient-specific computational phantoms together with clinical CT images of corresponding patients. Each patient-specific computational model includes 35 maternal organs and 25 foetal organs (Supplemental Table S1). The uterus of the patient-specific computational phantoms including the embedded foetus and other tissues were adjusted using rigid registration to the uterus region from patients' CT images. The uterus of the standardised phantom, including the foetus, was moved and scaled to fit the centroid and size of patient's uterus while the foetus was set in a head-down position.

CT source model

Monte Carlo-based techniques were used to create a previously validated GE 750HD CT source and CT gantry geometry models [32]. This CT scanner was equipped with Performix Pro VCT 100 x-ray tube with a 56° fan-beam angle, 7° target angle and allows for a beam collimation of 40 mm. The quality equivalent filtration of the x-ray tube is calculated at a nominal thickness value of 4.3 mm of aluminium at 120 kVp. The measured half-value layer was 7.8 mm Al at 120 kVp. The source to isocentre distance on this CT scanner is 54 cm, while the source to detector distance is 95 cm. The scanner's x-ray energy spectrum was generated using SpekCalc [33] and described as a function of the number of photons per kiloelectronvolt (keV) energy intervals in the Monte Carlo code. The Teflon bowtie filter and beam collimation were also included in the CT gantry model [32].

Monte Carlo simulations

The CT source model and computational models were integrated in the MCNPX code [34]. The simulated low-dose CT examinations were performed using the same parameters used for patients' scanning with a helical source path and total collimation width of 64×0.625 mm. Simulations of x-ray photon transport were performed in the CT model using all 30 patient-specific computational phantoms as input. The energies deposited in the 35 maternal organs and 25 foetal organs were recorded. The simulations for each helical CT scan were repeated six times with the tube starting angle differing by 60° because of the unknown tube- starting angles in the actual examinations. The foetal tissue compositions were obtained from ICRP 89 [35] with the bone density set to 1.3g/cm^3, whereas is was 0.99g/cm^3 for soft tissue.

Experimental measurements and simulations of absorbed dose

To calibrate the developed CT model and Monte Carlo simulation code, a series of dose measurements and

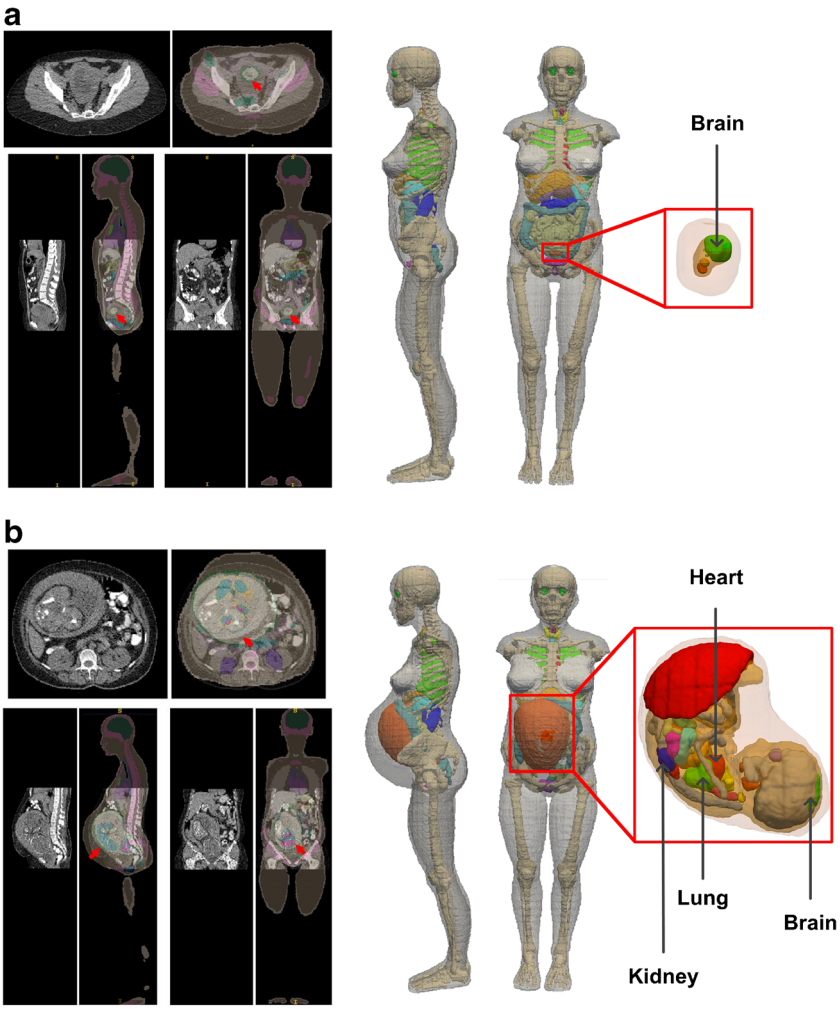

Fig. 2 Representative slices showing transverse (top), sagittal (bottom and left) and coronal (bottom and right) views of two examples of the developed computational phantoms at (**A**) 8 and (**B**) 35 weeks gestational age illustrating image registration between abdominal CT images of the patient and the computational phantom for the development of patient-specific pregnant computational models. A zoomed view of the 3D patient-specific pregnant computational models with the embedded foetus is also shown

simulations involving spiral CT scanning were performed in air using a 10-cm RaySafe™ Solo pencil chamber (Unfors RaySafe GmbH, Germany). The measurements were performed by positioning the ion chamber at the isocentre of the CT scanner with the long axis aligned with the axis of the CT gantry rotation. CT examinations were performed on the active volume of the detector, and the energy deposited in its air cavity was obtained and recorded as $D_{measured,\,in\,air}$. Monte Carlo simulations were then performed for the detector in air under the same geometrical conditions. The simulated free-in-air exposure value of the ion chamber was recorded as $D_{simulated,\,in\,air}$. The ratio of the measured to the simulated in-air dose refers to the conversion coefficient from simulated results to physical absolute dose and is defined as the output correction factor (OCF) [36]:

$$\mathrm{OCF} = \frac{D_{measured,in\ \ air}}{D_{simulated,in\ \ air}} \tag{1}$$

In this study, the measured and simulated free-in-air doses at 120 kVp tube voltage were 33.8 mGy/100 mAs

Table 1 Comparison between Monte Carlo simulated and measured radiation doses in head and body CT dosimetry phantoms

120 kVp tube voltage with a collimation of 40 mm	Head phantom	Body phantom
Absorbed dose per photon ($\times 10^{-15}$ mGy)	18.80	6.64
Number of photons ($\times 10^{12}$/Angle.mAs)	1.52	1.26
Simulated dose (mGy/100 mAs)	19.90	5.80
Measured dose (mGy/100 mAs)	19.90	6.00
Percent difference (%)	0.03	-3.50

and 4.8 mGy/100 mAs, respectively, with a calculated OCF value of 3.5.

To validate Monte Carlo-based dosimetric calculations, additional radiation dose measurements and simulations in similar conditions were performed using the head (16 cm diameter) and body (32 cm diameter) CT dosimetry phantoms made of polymethylmethacrylate. The measurements were performed by positioning the ion chamber at the centre of the cylindrical phantoms to obtain measured absorbed doses of $D_{measured,head}$ and $D_{measured,body}$, respectively, after performing CT examinations along the length of the cylindrical phantoms. To include the scatter tails at the beginning and the end of CT scans of the CTDI phantom, the 5-cm axial field of view (FOV) was set along the centre of the 10-cm pencil chamber. The absorbed doses in the computerised CT dosimetry phantoms were calculated as:

$$D_{estimated} = d_{simulated} \times n \times \Omega \times mAs \times OCF, \quad (2)$$

where $d_{simulated}$ is the absorbed dose per photon emitted from the source obtained in simulations, n is the number of photons emitted from the source per solid beam angle per mAs, calculated from *SpekCalc* [33] simulated x-ray energy spectra, Ω is the solid angle of the fan beam, *mAs* is the effective tube current-time product value and *OCF* is the estimated output correction factor. The dose was reported both in mGy and normalised to $CTDI_{vol}$.

Absorbed dose calculations for pregnant patients and foetus

The energy deposited in organs and tissues of the mother and foetus were recorded in the Monte Carlo code and used to

Table 2 Patient anatomical measurements together with the $CTDI_{vol}$-normalised foetal total-body dose (mGy/$CTDI_{vol}$) according to gestational age for the 30 pregnant patients involved in this study

Gestation age (week)	Conceptus depth (cm)	Maternal perimeter (cm)	Water-equivalent diameter (cm)	Dice coefficients	Jaccard coefficient	$CTDI_{vol}$-normalised foetal dose
8	13.9	126.2	34.1	0.96	0.55	1.11
8	18.1	92.5	25.9	0.94	0.63	0.85
8	13.8	97.9	24.1	0.93	0.60	1.06
8	15.3	104.0	29.6	0.96	0.65	1.08
8	16.0	109.8	28.0	0.95	0.64	0.97
8	13.4	98.5	27.0	0.92	0.61	1.31
8	13.6	97.6	24.5	0.94	0.54	1.17
8	13.8	97.4	25.2	0.97	0.64	1.27
10	15.8	105.7	27.6	0.94	0.58	1.26
10	14.7	102.5	26.9	0.95	0.62	1.34
10	19.4	127.9	37.5	0.96	0.64	0.93
12	20.3	96.1	26.6	0.94	0.65	1.08
15	15.9	105.0	26.7	0.95	0.64	1.63
16	17.5	112.7	30.8	0.96	0.65	1.12
17	16.6	97.0	26.8	0.94	0.58	1.41
18	15.2	89.3	24.8	0.96	0.57	1.55
21	15.8	95.7	28.0	0.94	0.58	1.36
22	12.9	106.7	29.8	0.96	0.56	0.98
22	18.7	110.6	29.0	0.95	0.58	1.23
25	18.2	110.4	28.2	0.95	0.57	1.07
25	17.5	107.4	27.5	0.94	0.51	1.08
25	20.6	115.8	31.7	0.96	0.56	1.01
26	19.8	124.4	35.7	0.95	0.56	1.16
26	20.3	120.5	31.7	0.96	0.55	1.20
28	17.7	104.9	26.7	0.96	0.49	1.23
29	18.1	113.7	27.3	0.95	0.45	1.08
30	18.4	105.7	27.9	0.93	0.53	1.23
32	20.8	122.8	34.5	0.95	0.48	0.92
35	20.3	120.6	29.7	0.97	0.54	0.95
35	19.7	111.7	30.4	0.93	0.58	1.20

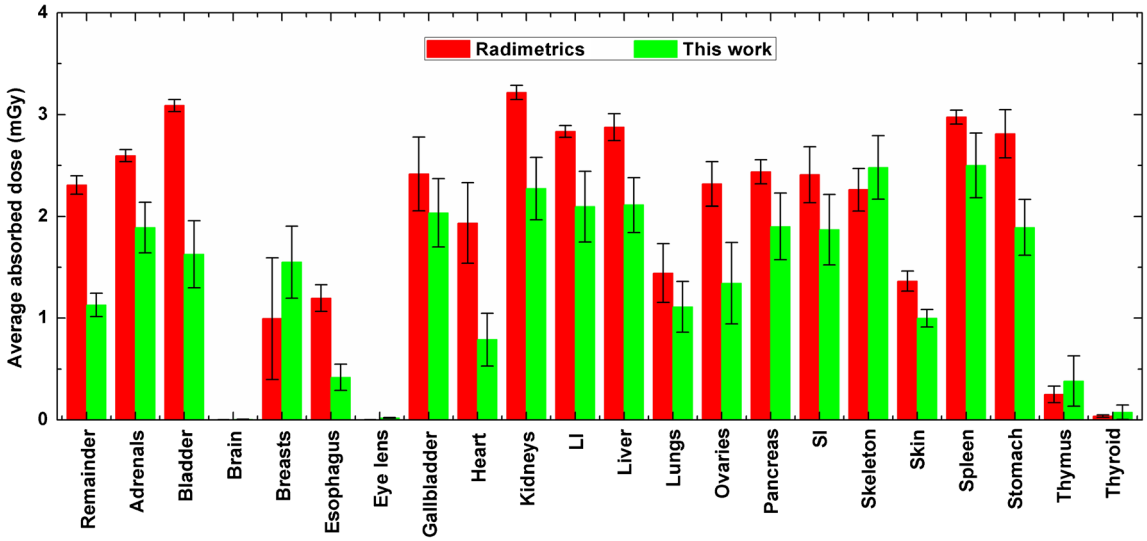

Fig. 3 Comparison between absorbed doses to maternal organs estimated using Monte Carlo calculations and Radimetrics™ dose-tracking system

calculate the absorbed dose of each organ and tissue from clinical CT scans according to Eq. (2). The effective dose was calculated according to the ICRP recommendations [37]:

$$E = \sum_T \omega_T \sum_R \omega_R D_{R,T}, \quad (3)$$

where E is the effective dose, ω_R is the radiation weighting factor for radiation type R, $D_{R,T}$ is the contribution of radiation type R to the absorbed dose, and ω_T is the tissue weighting factor for organ or tissue T reflecting its relative radiation sensitivity [37]. Since the effective dose recommended by the ICRP provides protection quantity for the whole population, the effective dose for the pregnant patient was calculated based on estimated maternal organ absorbed doses.

Subsequently, clinical CT images for each patient were imported into Radimetrics™ dose-tracking software [30] for calculation of maternal effective dose. Radimetrics™ collects CT scans directly from the hospital's picture archiving and communication system and matches patient images with Cristy & Eckerman stylised computational phantoms [38] according to age, gender, weight and body size (as shown in Supplemental Fig. S1). The software extracts scanning parameters (tube voltage, mAs, scan range, etc.) from the DICOM files' header information and calculates patient-specific absorbed dose at the organ level using Monte Carlo simulations.

The results obtained by Radimetrics™ and the effective dose calculated by multiplying the dose-length product (DLP) of CT examinations by appropriate conversion factors [39] were considered as reference values in this work. The results obtained using the patient-specific computational model and Monte Carlo calculations were further compared with these reference values [28]. This assumption is justified by the large number of users reporting on the validation of the MCNPX code and the more realistic computational models used in this work compared to stylised models adopted by Radimetrics™.

The absolute foetal dose is given in mGy for comparison between the results of this work and those reported in the literature. However, since the absolute foetal dose is scanner dependent, the $CTDI_{vol}$-normalised-organ dose coefficient [40] was obtained by multiplying the foetal dose by the effective mAs and dividing the result by the $CTDI_{vol}$ (1.8 mGy) to normalise based on $CTDI_{vol}$, which has been demonstrated to be effectively independent of the CT scanner [41].

Statistical analysis

The correlations between foetal organ doses for the cohort included in the study protocol and the three variables, namely gestational age, conceptus depth and maternal perimeter, were tested using SPSS [42]. Pearson correlation coefficients were calculated to determine statistical significance. Nonlinear curve-fitting was performed to assess the absorbed dose of foetal organs as a function of the three parameters (gestational age, conceptus depth and maternal perimeter) presenting with high and significant correlation (the Pearson correlation is significant at the 0.05 level).

Results

Validation of the Monte Carlo code

Table 1 compares the measured and Monte Carlo-simulated radiation doses in head and body CT dosimetry phantoms scanned on the Discovery CT 750HD CT scanner at 120

kVp with a collimation of 40 mm. The differences between measured and simulated absorbed doses for the head and body CT dosimetry phantoms are 0.03% and −3.5%, respectively.

Patient-specific computational phantoms

The results of automated thresholding-based segmentation were compared with manual segmentation of all CT images with respect to the outline, skeleton and lungs. The Dice similarity coefficient [43] between the two methods varied between 0.92 to 0.97 with an average of 0.95 ± 0.01 (Table 2). The accuracy of the registration between the regional models of pregnant patients and the patient-specific computational models was evaluated by calculating Jaccard's coefficient of similarity [43]. The latter varies between 0.45 and 0.65 with an average of 0.58 ± 0.05 among patients.

Absorbed and effective doses to pregnant patients

The absorbed doses of maternal organs were calculated for all patients according to Eqs. (2) and (3) using Monte Carlo simulations. Figure 3 compares the average absorbed dose for different maternal organs with estimates provided by the Radimetrics™ commercial dose-tracking system. The results provided by the commercial software are a bit different from our simulations but still in the same order of magnitude. For organs located in the region covered by abdominal and pelvic CT scans, the differences between simulated results and absorbed doses reported by Radimetrics™ dose-tracking software range between −47% and −16%. The organs located outside the acquisition FOV for abdominal CT scans, such as the brain, eye lens and thyroid etc., receive a significantly lower dose than other organs.

The effective doses for the 30 pregnant patients varied between 1.1 mSv and 2.0 mSv, with an average of 1.6 ± 0.22 mSv, while Radimetrics™ reported an effective dose ranging between 1.7 mSv and 2.3 mSv with an average of 1.9 ± 0.14 mSv. The effective doses calculated using the DLPs and corresponding conversion factors of Huda et al.[39] range between 1.5 mSv and 1.9 mSv, with an average of 1.6 ± 0.11 mSv.

CT foetal dose

Table 2 summarises the calculated foetal doses normalised to $CTDI_{vol}$ according to gestational age of pregnant patients. The water-equivalent diameter [41] of the pregnant patients varies between 24.1 cm and 37.5 cm. The measurements of conceptus depth and maternal perimeter, which vary from 12.9 cm to 20.8 cm and 89.3 cm to 127.9 cm, respectively, are also shown. Table 3 compares the normalised foetal body doses with results reported in the literature. The average absolute dose to different foetal organs from CT examinations ranges between 1.12 mGy and 5.98 mGy (Table 4). The scanner independent $CTDI_{vol}$-normalised foetal organ dose coefficients are shown in Table 4. The foetus brain and bone marrow receive an average dose of 3.11 ± 1.09 mGy and 1.44 ± 0.45 mGy, respectively.

The foetal total body dose is about 2.11 ± 0.37 mGy while Radimetrics™ reported 2.47 ± 0.42 mGy. The $CTDI_{vol}$-normalised organ dose coefficients [40] of foetal organs vary between 0.62 and 3.32. Figure 4 shows the ratios of absorbed doses to the foetal body between the values estimated using Monte Carlo simulations and Radimetrics™. The average absolute differences of foetal doses between Monte Carlo simulations and Radimetrics™ are about 21%.

This study presents, for the first time, detailed organ-level radiation doses to the foetus from CT examinations. Figure 5 shows the average normalised absorbed dose of different foetal organs from CT examinations. It can be observed that the absorbed dose is non-uniformly distributed between foetal organs where the foetal skeleton and bone marrow receive about 3.8 and 2.0 times higher absorbed doses, respectively, than other foetal tissues. Pearson correlation coefficients between foetal organ doses and the three independent parameters (conceptus depth, maternal perimeter and gestational age) are summarised in Table 5. As shown in Fig. 6, linear regression analysis indicated no significant correlation between foetal

Table 3 Comparison of foetal total-body absorbed doses from CT scans of pregnant patients between this study and results reported in the literature

		This study	Felmlee et al. [44]	Angel et al. [11]	Damilakis et al. [12]	Gu et al. [21]
No. of patient models		30	1	24	117	3
Foetal dose per 100 mAs (mGy/100 mAs)	Average ± SD	9.20 ± 1.60	11.30	10.80 ± 1.80	22.60	6.60 ± 1.60
	Range	6.70 - 13.0	9.00 - 13.60	7.30 - 14.30	13.50 - 31.60	4.90 - 8.80
Foetal dose normalised per $CTDI_{vol}$ (mGy/$CTDI_{vol}$)	Average ± SD	1.17 ± 0.20	-	-	-	1.40 ± 0.60
	Range	0.85 - 1.63	-	-	-	0.84 - 2.22
Averaged foetal organ dose per $CTDI_{vol}$ (mGy/$CTDI_{vol}$)	Soft tissue	0.94 ± 0.17	-	-	-	1.29 ± 0.46
	Skeleton	3.32 ± 0.92	-	-	-	4.47 ± 0.88
	Brain	0.80 ± 0.25	-	-	-	1.00 ± 0.26

Table 4 Average absolute and $CTDI_{vol}$-normalised foetal organ doses (organ dose/$CTDI_{vol}$) for different foetal organs for the 30 patients

Foetal organs	Average absolute foetal organ dose (mGy)	$CTDI_{vol}$-normalised foetal organ dose
Adrenal	1.67 ± 0.29	0.93 ± 0.16
Bone marrow	3.11 ± 1.09	1.73 ± 0.61
Brain	1.44 ± 0.45	0.80 ± 0.25
Oesophagus	1.37 ± 0.27	0.76 ± 0.15
Eyes	1.12 ± 0.31	0.62 ± 0.17
Gall bladder	1.62 ± 0.24	0.90 ± 0.13
Heart	1.66 ± 0.34	0.92 ± 0.19
Kidneys	1.87 ± 0.30	1.04 ± 0.17
LI	1.65 ± 0.27	0.92 ± 0.15
Liver	1.78 ± 0.31	0.99 ± 0.17
Lungs	1.70 ± 0.31	0.94 ± 0.17
Pancreas	1.73 ± 0.30	0.96 ± 0.17
SI	1.69 ± 0.26	0.94 ± 0.14
Skeleton	5.98 ± 1.66	3.32 ± 0.92
Skin	1.70 ± 0.31	0.94 ± 0.17
Salivary gland	1.17 ± 0.29	0.65 ± 0.16
Soft tissue	1.70 ± 0.31	0.94 ± 0.17
Spinal cord	1.67 ± 0.28	0.93 ± 0.16
Spleen	1.83 ± 0.28	1.02 ± 0.16
Stomach	1.72 ± 0.30	0.96 ± 0.17
Testis	1.50 ± 0.21	0.83 ± 0.12
Thymus	1.36 ± 0.26	0.76 ± 0.14
Thyroid	1.51 ± 0.41	0.84 ± 0.23
UB	1.72 ± 0.29	0.96 ± 0.16
Total body	2.11 ± 0.37	1.17 ± 0.21

total body dose and gestational age, while significant correlations were observed between foetal total body dose and the conceptus depth or maternal size. For the foetal brain, the correlation coefficients between absorbed dose and the gestational age, conceptus depth and maternal size are −0.83, −0.71 and −0.58, respectively, indicating a significant correlation between foetal brain dose and the above parameters. The absorbed doses to some organs, such as the kidney, gall bladder, large intestine (LI), small intestine (SI), urinary bladder (UB), etc., present insignificant correlations with both gestational age and conceptus depth. The foetal organ absorbed dose as a function of the anatomical and physiological parameters presenting with high correlations is parameterised using nonlinear curve-fittings (Table 5).

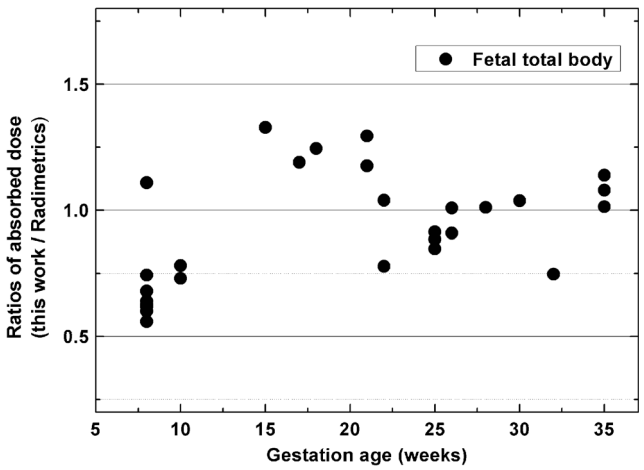

Fig. 4 Ratios of absorbed doses to the foetal body between Monte Carlo calculations and Radimetrics™ dose-tracking system

Discussion

We implemented a methodological framework for assessment of patient-specific foetal dose suitable for application in clinical setting. Pregnant patients with a range of anatomical variability undergoing CT examinations can be adapted by segmenting CT images to produce a voxelised regional model and registering it to a standardised computational model to construct a patient-specific CT scan model suitable for incorporation in a dedicated Monte Carlo code. The radiation dose to the foetal body from

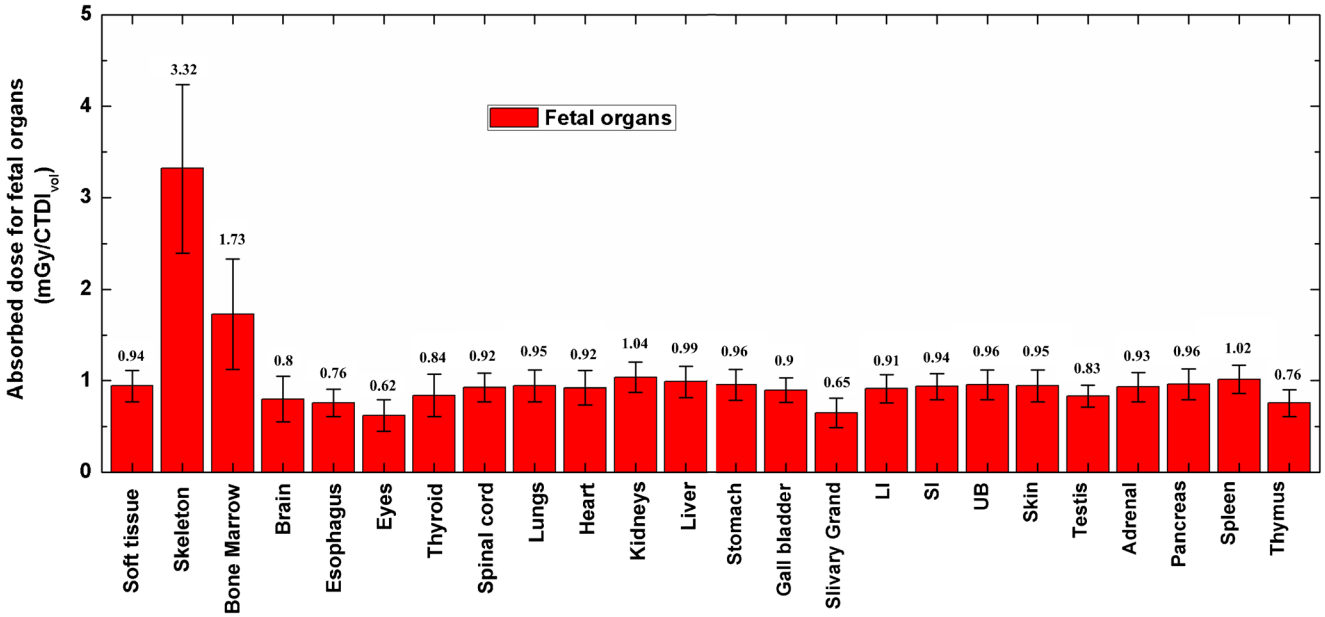

Fig. 5 Normalised absorbed doses of foetal organs from CT scans performed on pregnant patients with the average values for each organ

CT examinations of pregnant patients varies within the range 6.7–13 mGy/100 mAs with a mean value of 9.2 mGy, while Felmlee et al. [44], Angel et al. [11], Damilakis et al. [12] and Gu et al. [21] reported foetal doses of 11.3 mGy/100 mAs (Picker 1200, Siemens DRH, GE 9800 and GE 8800), 10.8 mGy/100 mAs (GE HighSpeed CT/I, GE LightSpeed QX/i, GE LightSpeed Ultra, GE LightSpeed PRO, GE LightSpeed 16 and GE LightSpeed VCT), 22.6 mGy/100 mAs (Siemens Sensation 16 CT scanner) and 6.6 mGy/100 mAs (GE LightSpeed Pro16 and GE LightSpeed™ 16), respectively. The foetal doses normalised to $CTDI_{vol}$ were 1.17, 0.94, 3.32 and 0.80 for the body, soft tissue, skeleton and brain, respectively. The corresponding body and organ foetal doses reported by Gu et al. [21] are 1.4, 1.29, 4.47 and 1.00, respectively. The radiosensitivity and radiation risks of the developing foetal organs vary across the different trimesters or gestational age. Therefore, the study of correlations between radiation exposure to conceptus and organ-specific childhood cancer after birth requires estimation of organ-level radiation dose to the foetus. However, the foetal organ-level radiation dose from CT examinations is rarely reported in literature. In this work, the absorbed doses to 25 foetal organs were evaluated for pregnant patients undergoing CT examinations. The average foetal organ dose normalised to $CTDI_{vol}$ varies between 0.62 and 3.32 (Fig. 5). The absorbed dose is non-uniformly distributed within the different foetal organs. The foetal skeleton and bone marrow receive significantly higher absorbed dose than other soft tissues because the high density of bones results in higher energy deposition in the skeleton. Since radiation exposure of bone marrow and brain in childhood may increase the risk of leukaemia and brain tumours [10], the absorbed dose to foetal bone marrow and foetal brain during CT examinations of pregnant patients is an important matter of concern for the radiologist and the patient.

This work compares Monte Carlo simulated radiation doses with estimates reported by a commercial dose-tracking system, conventional DLP-based absorbed doses and results reported in the literature. Our results are in agreement with observations reported elsewhere confirming that the foetal total body dose has significant correlations with patient size but insignificant correlation with gestational age [11]. However, the absorbed radiation dose of the foetal brain shows significant correlations with patient size, conceptus depth and gestational age while some foetal organs, such as the kidneys, large intestine (LI), small intestine (SI), spleen, urinary bladder (UB), etc., present significant correlations with patient size but insignificant correlation with conceptus depth and gestational age.

Three main factors contribute to the uncertainty on the calculated foetal dose: segmentation of clinical CT images (<5%), image registration of the computational phantom to the clinical CT scan (<30%), which determines the accuracy of the represented anatomical geometry of the patient, and the Monte Carlo calculation uncertainty (<2%), which can be reduced by increasing the simulated particle histories.

The obtained normalised absorbed dose can be used for estimating foetal dose for pregnant patients undergoing CT examinations at other tube current-time product settings since higher mAs values are commonly used to scan

Table 5 Pearson correlation coefficients between foetal organ doses of the cohort and the three parameters (gestational age, conceptus depth and maternal perimeter). Nonlinear curve-fitting was used to estimate the foetal organ dose as a function of the three parameters presenting with significant correlation at the 0.01 level using a two-tailed statistical test. The R^2 values for the non-linear curve-fitting are also shown

Foetal organs	Pearson correlation coefficient			Dose functions (mGy/$CTDI_{vol}$)	R^2
	Conceptus depth	Maternal perimeter	Gestation age		
Total body	−0.37*	−0.53*	−0.06	Dose = 2.265–0.01(De)–0.0086(Pr)	0.29
Soft tissue	−0.66*	−0.65*	−0.59*	Dose = 2.07–0.016(De)–0.007(Pr)–0.0056(Ag)	0.60
Skeleton	−0.72*	−0.59*	−0.75*	Dose = 9.053–0.089(De)–0.028(Pr)–0.058(Ag)	0.75
Bone marrow	−0.71*	−0.54*	−0.84*	Dose = 5.067–0.039(De)–0.015(Pr)–0.0486(Ag)	0.81
Brain	−0.71*	−0.58*	−0.83*	Dose = 2.063–0.019(De)–0.0058(Pr)–0.0174(Ag)	0.79
Oesophagus	−0.40	−0.71*	−0.25	Dose = 1.866–0.01(Pr)	0.50
Eyes	−0.48*	−0.76*	−0.71*	Dose = 1.826–0.01(De)–0.01(Pr)–0.012(Ag)	0.73
Thyroid	−0.68*	−0.70*	−0.76*	Dose = 2.16 + 0.03(De)–0.0126(Pr)–0.02(Ag)	0.71
Spinal cord	−0.34	−0.63*	−0.16	Dose = 1.94–0.009(Pr)	0.39
Lung	−0.65*	−0.58*	−0.53*	Dose = 2.027–0.027(De)–0.005(Pr)–0.0033(Ag)	0.52
Heart	−0.71*	−0.61*	−0.62*	Dose = 2.12–0.03(De)–0.0055(Pr)–0.0056(Ag)	0.62
Kidney	−0.25	−0.53*	0.13	Dose = 1.946–0.0083(Pr)	0.28
Liver	−0.63*	−0.58*	−0.44*	Dose = 2.1–0.0315(De)–0.0053(Pr)–0.0006(Ag)	0.48
Stomach	−0.62*	−0.58*	−0.43*	Dose = 2.042–0.03(De)–0.0053(Pr)–0.0006(Ag)	0.47
Gall bladder	−0.36	−0.58*	−0.30	Dose = 1.747–0.0078(Pr)	0.34
Salivary grand	−0.49*	−0.72*	−0.76*	Dose = 1.674 + 0.012(De)–0.0086(Pr)–0.0133(Ag)	0.74
LI	−0.40	−0.73*	−0.44	Dose = 2.116–0.011(Pr)	0.54
SI	−0.40	−0.62*	−0.38	Dose = 1.894–0.0088(Pr)	0.38
UB	−0.33	−0.71*	−0.07	Dose = 2.153–0.011(Pr)	0.50
Skin	−0.67*	−0.61*	−0.54*	Dose = 2.061–0.028(De)–0.0054(Pr)–0.0032(Ag)	0.56
Testis	−0.22	−0.62*	−0.35	Dose = 1.741–0.0082(Pr)	0.38
Adrenal	−0.29	−0.52*	−0.03	Dose = 1.789–0.0079(Pr)	0.27
Pancreas	−0.59*	−0.54*	−0.37*	Dose = 2.022–0.032(De)–0.0049(Pr)–0.0009(Ag)	0.42
Spleen	−0.31	−0.63*	−0.41	Dose = 2.065–0.0096(Pr)	0.40
Thymus	−0.48*	−0.71*	−0.52*	Dose = 1.787 + 0.0064(De)–0.009(Pr)–0.0069(Ag)	0.60

* Correlation is significant at the 0.05 level (2-tailed)

De conceptus depth (in cm), *Pr* maternal perimeter (in cm), *Ag* gestational age (in weeks)

heavy or large patients. We are actually expanding the capabilities of the developed framework to other patient populations and different CT scanner models.

The mean foetal total body dose estimated in this work for the investigated patient cohort is consistent with results reported in the literature, but is about 14% lower than the estimates provided by Radimetrics™ dose-tracking system. This discrepancy may be attributed to the utilisation of simplistic stylised pregnant female phantoms and many other approximations and assumptions made by Radimetrics™, which results in an overestimation of the foetal dose.

Among the limitations of this study is that the foetus in the standard pregnant phantoms is facing the downward position while the actual foetal position may vary among patients. This posture variation may affect the dose distributions in foetal organs from CT scan and bring uncertainties in the dose estimation. Another limitation related to the development of patient-specific computational models is the requirement of manual segmentation of the uterus region, which increases the workload for achieving pregnant patient-specific radiation dosimetry. The computation time depends on the number of simulated particles (about 7 min for 2 million simulated photons), the choice of the latter is related to the desired accuracy of the estimates or statistical uncertainty. Overall, the computational time is of the order of 14 h on a single core of Intel Xeon CPU E5-2630 to get less than 2% coefficient of variation. With advances in computer technology, the proposed approach could be implemented in the clinic by subdividing time-consuming simulations on a cluster of computer nodes or geographically distributed platforms taking advantage of the latest developments in grid technology.

Overall, the foetal doses were significantly lower than the consensus level for negligible risks (50 mGy) for

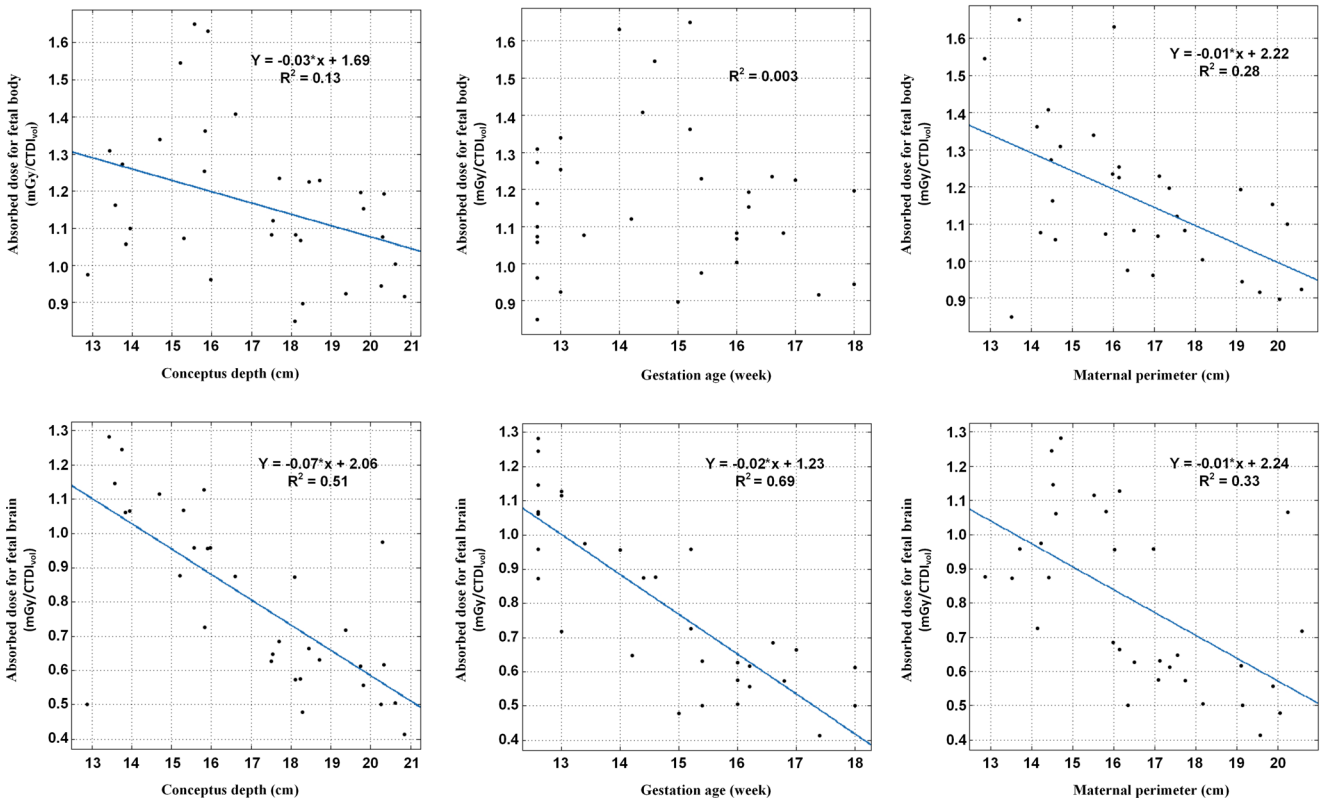

Fig. 6 Plots of radiation dose to the foetal body and foetal brain versus conceptus depth, gestational age and maternal perimeter. No significant correlation was observed between foetal total-body dose and gestational age

deterministic effects. Still, ample justification to perform CT scans for pregnant patients and adequate documentation of the lack of alternative options is still necessary. Since patient size has a noticeable effect on foetal dose estimates, this work shows that patient-specific computational models can be created based on the available standardised computational phantoms of pregnant females to reflect personalised body morphometries. This enables radiologists to perform patient-specific dosimetry for a variety of radiation exposure situations and provide elaborate estimation of organ-level radiation dose to the foetus.

Compliance with ethical standards

Guarantor The scientific guarantor of this publication is Habib Zaidi.

Conflict of interest The authors of this manuscript declare no relationships with any companies whose products or services may be related to the subject matter of the article.

Funding This study has received funding from the Swiss National Science Foundation under Grant SNSF 31003A-149957.

Statistics and biometry No complex statistical methods were necessary for this paper.

Informed consent Written informed consent was waived by the Institutional Review Board.

Ethical approval Institutional Review Board approval was obtained.

Methodology
- retrospective
- experimental
- performed at one institution

References

1. Lazarus E, DeBenedectis C, North D, Spencer PK, Mayo-Smith WW (2009) Utilization of Imaging in Pregnant Patients: 10-year Review of 5270 Examinations in 3285 Patients—1997–2006 1. Radiology 251:517–524
2. Xie T, Zaidi H (2014) Fetal and maternal absorbed dose estimates for positron-emitting molecular imaging probes. J Nucl Med 55: 1459–1466
3. Zanotti-Fregonara P, Laforest R, Wallis JW (2015) Fetal radiation dose from [18F]-FDG in pregnant patients imaged with PET, PET/CT and PET/MRI. J Nucl Med 56:1218–1222
4. Azim Jr HA (Ed) (2016) Managing Cancer During Pregnancy. Springer
5. American College of Radiology. ACR-SPR Practice Parameter for Imaging Pregnant or Potentially Pregnant Adolescents and Women with Ionizing Radiation. Revised 2013 (Resolution 48). Availble at http://www.acr.org/~/media/ACR/Documents/PGTS/guidelines/Pregnant_Patients.pdf

6. ICRP Publication 84 (2000) Pregnancy and medical radiation. Ann ICRP 30:1–43
7. ICRP Publication 90 (2003) Biological effects after prenatal irradiation (embryo and fetus). Ann ICRP 33:5–206
8. Altman KI, Lett JT (2013) Relative radiation sensitivities of human organ systems. Elsevier
9. McCollough CH, Schueler BA, Atwell TD et al (2007) Radiation Exposure and Pregnancy: When Should We Be Concerned? Radiographics 27:909–917
10. Pearce MS, Salotti JA, Little MP et al (2012) Radiation exposure from CT scans in childhood and subsequent risk of leukaemia and brain tumours: a retrospective cohort study. Lancet 380:499–505
11. Angel E, Wellnitz CV, Goodsitt MM et al (2008) Radiation Dose to the Fetus for Pregnant Patients Undergoing Multidetector CT Imaging: Monte Carlo Simulations Estimating Fetal Dose for a Range of Gestational Age and Patient Size 1. Radiology 249:220–227
12. Damilakis J, Perisinakis K, Tzedakis A, Papadakis AE, Karantanas A (2010) Radiation Dose to the Conceptus from Multidetector CT during Early Gestation: A Method That Allows for Variations in Maternal Body Size and Conceptus Position 1. Radiology 257:483–489
13. Damilakis J, Tzedakis A, Perisinakis K, Papadakis AE (2010) A method of estimating conceptus doses resulting from multidetector CT examinations during all stages of gestation. Med Phys 37:6411–6420
14. Gilet AG, Dunkin JM, Fernandez TJ, Button TM, Budorick NE (2011) Fetal radiation dose during gestation estimated on an anthropomorphic phantom for three generations of CT scanners. Am J Roentgen 196:1133–1137
15. Helmrot E, Pettersson H, Sandborg M, Altén JN (2007) Estimation of dose to the unborn child at diagnostic X-ray examinations based on data registered in RIS/PACS. Eur Radiol 17:205–209
16. Hoseinian-Azghadi E, Rafat-Motavalli L, Miri-Hakimabad H (2014) Development of a 9-months pregnant hybrid phantom and its internal dosimetry for thyroid agents. J Radiat Res 55:730–747
17. Lopez-Rendon X, Walgraeve M, Woussen S et al (2017) Comparing different methods for estimating radiation dose to the conceptus. Eur Radiol 27:851–858
18. Maynard MR, Long NS, Moawad NS et al (2014) The UF Family of hybrid phantoms of the pregnant female for computational radiation dosimetry. Phys Med Biol 59:4325–4343
19. Winer-Muram HT, Boone JM, Brown HL, Jennings SG, Mabie WC, Lombardo GT (2002) Pulmonary Embolism in Pregnant Patients: Fetal Radiation Dose with Helical CT 1. Radiology 224:487–492
20. Myronakis M, Perisinakis K, Tzedakis A, Gourtsoyianni S, Damilakis J (2009) Evaluation of a patient-specific Monte Carlo software for CT dosimetry. Radiat Protect Dosimetry 133:248–255
21. Gu J, Xu XG, Caracappa PF, Liu B (2012) Fetal doses to pregnant patients from CT with tube current modulation calculated using Monte Carlo simulations and realistic phantoms. Radiat Protect Dosimetry 155:64–72
22. Chatterson LC, Leswick DA, Fladeland DA, Hunt MM, Webster S, Lim H (2014) Fetal shielding combined with state of the art CT dose reduction strategies during maternal chest CT. Eur J Radiol 83:1199–1204
23. Jaffe TA, Neville AM, Anderson-Evans C et al (2009) Early first trimester fetal dose estimation method in a multivendor study of 16- and 64-MDCT scanners and low-dose imaging protocols. Am J Roentgen 193:1019–1024
24. Jaffe TA, Yoshizumi TT, Toncheva GI, Nguyen G, Hurwitz LM, Nelson RC (2008) Early first-trimester fetal radiation dose estimation in 16-MDCT without and with automated tube current modulation. Am J Roentgen 190:860–864
25. Kelaranta A, Kaasalainen T, Seuri R, Toroi P, Kortesniemi M (2015) Fetal radiation dose in computed tomography. Radiat Protect Dosimetry 165:226–230
26. Solomou G, Papadakis A, Damilakis J (2015) Abdominal CT during pregnancy: a phantom study on the effect of patient centring on conceptus radiation dose and image quality. Eur Radiol 25:911–921
27. Zaidi H, Xu XG (2007) Computational anthropomorphic models of the human anatomy: The path to realistic Monte Carlo modeling in medical imaging. Annu Rev Biomed Eng 9:471–500
28. Zaidi H, Ay M (2007) Current status and new horizons in Monte Carlo simulation of X-ray CT scanners. Med Biol Eng Comput 45:809–817
29. Xie T, Zaidi H (2016) Development of computational pregnant female and fetus models and assessment of radiation dose from positron-emitting tracers. Eur J Nucl Med Mol Imaging 43:2290–2300
30. Radimetrics Enterprise Platform: Dose Management Solution. Bayer HealthCare. http://www.radiologysolutions.bayer.com/products/ct/dosemanagement/rep/. (Accessed 2016)
31. Ibanez L, Schroeder W, Ng L, Cates J (2005) The ITK software guide. http://hdl.handle.net/1926/388
32. Akbarzadeh A, Ay MR, Ghadiri H, Sarkar S, Zaidi H (2010) Measurement of scattered radiation in a volumetric 64-slice CT scanner using three experimental techniques. Phys Med Biol 55:2269–2280
33. Poludniowski G, Landry G, DeBlois F, Evans P, Verhaegen F (2009) SpekCalc: a program to calculate photon spectra from tungsten anode x-ray tubes. Phys Med Biol 54:N433–N438
34. Pelowitz DB (2005) MCNPX User's Manual Version 2.5.0. Los Alamos National Laboratory, Los Alamos
35. ICRP (2002) Basic anatomical and physiological data for use in radiological protection: reference values: ICRP Publication 89. Ann ICRP 32:1–277
36. Li X, Samei E, Segars WP et al (2011) Patient-specific radiation dose and cancer risk estimation in CT: Part I. Development and validation of a Monte Carlo program. Med Phys 38:397–407
37. ICRP (2007) ICRP Publication 103: The 2007 Recommendations of the International Commission on Radiological Protection. Ann ICRP 37:1–332
38. Cristy M, Eckerman KF (1987) Specific absorbed fractions of energy at various ages from internal photon sources. I Methods, II one year old, III five year old, IV ten year old, V fifteen year old male and adult female, VI new-born and VII adult male. Oak Ridge National Laboratory, Oak Ridge
39. Huda W, Ogden KM, Khorasani MR (2008) Converting dose-length product to effective dose at CT 1. Radiology 248:995–1003
40. Tian X, Li X, Segars WP, Paulson EK, Frush DP, Samei E (2014) Pediatric chest and abdominopelvic CT: organ dose estimation based on 42 patient models. Radiology 270:535–547
41. AAPM (2014) Use of water equivalent diameter for calculating patient size and size-specific dose estimates (SSDE) in CTCT (Task group 220). American Association of Physicists in Medicine, College Park
42. Norusis MJ (1992) SPSS for Windows: Professional Statistics User's Guide, Release 5.0. SPSS Incorporated
43. Jackson DA, Somers KM, Harvey HH (1989) Similarity coefficients: measures of co-occurrence and association or simply measures of occurrence? Am Nat 133:436–453
44. Felmlee JP, Gray J, Leetzow M, Price J (1990) Estimated fetal radiation dose from multislice CT studies. AJR Am J Roentgen 154:185–190